

# REPORT DOCUMENTATION PAGE

Form Approved  
OMB NO. 0704-0188

Public Reporting burden for this collection of information is estimated to average 1 hour per response, including the time for reviewing instructions, searching existing data sources, gathering and maintaining the data needed, and completing and reviewing the collection of information. Send comment regarding this burden estimates or any other aspect of this collection of information, including suggestions for reducing this burden, to Washington Headquarters Services, Directorate for information Operations and Reports, 1215 Jefferson Davis Highway, Suite 1204, Arlington, VA 22202-4302, and to the Office of Management and Budget, Paperwork Reduction Project (0704-0188,) Washington, DC 20503.

1. AGENCY USE ONLY ( Leave Blank)		2. REPORT DATE 08-16-2005	3. REPORT TYPE AND DATES COVERED Final Report: 8-1-2004 through 6-30-2005	
4. TITLE AND SUBTITLE Investigation of an Electromagnetic Induction Sensor			5. FUNDING NUMBERS W911NF-04-1-0255	
6. AUTHOR(S) Waymond R. Scott, Jr.				
7. PERFORMING ORGANIZATION NAME(S) AND ADDRESS(ES) Georgia Tech Research Institute Georgia Institute of Technology 505 Tenth Street, NW Atlanta, GA 30332-0420			8. PERFORMING ORGANIZATION REPORT NUMBER	
9. SPONSORING / MONITORING AGENCY NAME(S) AND ADDRESS(ES)  U. S. Army Research Office P.O. Box 12211 Research Triangle Park, NC 27709-2211			10. SPONSORING / MONITORING AGENCY REPORT NUMBER  4 7 1 1 5 . 1 - E V	
11. SUPPLEMENTARY NOTES The views, opinions and/or findings contained in this report are those of the author(s) and should not be construed as an official Department of the Army position, policy or decision, unless so designated by other documentation.				
12 a. DISTRIBUTION / AVAILABILITY STATEMENT  Approved for public release; distribution unlimited.			12 b. DISTRIBUTION CODE	
13. ABSTRACT (Maximum 200 words)  A new technique is presented for canceling the coupling between the coils of an electromagnetic induction sensor while using simple dipole detection coils. A secondary bucking transformer is used to cancel the coupling between the coils. The technique allows for the cancellation that can be obtained using a quadrupole receive coil while maintaining the depth sensitivity and simple detection zone of a dipole coil. Simple circuit models for the sensor with some of the important parasitic effects are developed. An experimental model is developed and used to demonstrate the technique. Experimental results are presented that demonstrate the effectiveness of this technique.				
14. SUBJECT TERMS Landmine Detection, EMI, Electromagnetic Induction, Metal Detector			15. NUMBER OF PAGES 14	
			16. PRICE CODE	
17. SECURITY CLASSIFICATION OR REPORT <b>UNCLASSIFIED</b>	18. SECURITY CLASSIFICATION ON THIS PAGE <b>UNCLASSIFIED</b>	19. SECURITY CLASSIFICATION OF ABSTRACT <b>UNCLASSIFIED</b>	20. LIMITATION OF ABSTRACT  <b>UL</b>	

NSN 7540-01-280-5500

**Standard Form 298 (Rev.2-89)**  
Prescribed by ANSI Std. Z39-18  
298-102

# **Final Report**

for the project

## **Investigation of an Electromagnetic Induction Sensor**

by

**Waymond R. Scott, Jr.**

Georgia Institute of Technology  
School of Electrical and Computer Engineering  
Atlanta, GA 30332-0250

ARO contract number W911NF-04-1-0255

### **ABSTRACT**

A new technique is presented for canceling the coupling between the coils of an electromagnetic induction sensor while using simple dipole detection coils. A secondary bucking transformer is used to cancel the coupling between the coils. The technique allows for the cancellation that can be obtained using a quadrupole receive coil while maintaining the depth sensitivity and simple detection zone of a dipole coil. Simple circuit models for the sensor with some of the important parasitic effects are developed. An experimental model is developed and used to demonstrate the technique. Experimental results are presented that demonstrate the effectiveness of this technique.

Keywords: Landmine Detection, EMI, Electromagnetic Induction, Metal Detector

## **Table of Contents**

Introduction	3
Approach	3
Experimental Results for Prototype #1	6
Experimental Results for Prototype #2	9
Sensitivity of Toroidal Transformer to External Metal Objects	12
Conclusions and Future Work	12
References	13
Personnel	14
Publications	14
Report of Inventions	14

## Introduction

For many years, extensive effort has been expended developing techniques for locating land mines. For a mine detection technique to be successful there must sufficient contrast between the properties of the mine and the earth. There also must be sufficient contrast between the properties of the mine and common types of clutter such as rocks, roots, cans, etc. so that the mine can be distinguished from the clutter. The latter condition is the most problematic for most mine detection techniques. For example, simple electromagnetic induction (EMI) sensors are capable of detecting most mines; however, they will also detect every buried metal object such as bottle tops, nails, shrapnel, bullets, etc. This results in an unacceptable false alarm rate. This is even more problematic for low-metal anti-personnel mines as they are extremely difficult to distinguish from clutter using a simple EMI sensor. In recent years, advanced EMI sensors that use a broad range of frequencies or a broad range of measurement times along with advanced signal processing have been shown to be capable of discrimination between buried land mines and many types of buried metal clutter [1-4]. For these advanced EMI sensors to be effective, they must be able to accurately, repeatably, and quickly measure the response of a buried target. This is difficult because the sensor must operate with bandwidths greater than 100 to 1 while accurately measuring signals that are more than 80 dB smaller than the direct coupling between the coils on the EMI sensor. In order to accomplish this, the EMI sensor must be very cleverly designed to account for the coupling and for the secondary effects such as resonances in the coils.

In most EMI sensors, the coupling between the coils is handled by one of two methods. In time-domain sensors, the coupling between the coils can be mostly removed by time gating if the coils are properly designed. In frequency domain sensors, the coupling is mostly removed by using a quadrupole receive coil which minimizes the mutual inductance between the coils. The coils are usually formed using one of three common forms. In the first form, the receive coil is wound in a figure 8 pattern. In the second form, two receive coils of the same size and numbers of turns are wound on the same axis and are spaced a distance apart. The two coils are wound in opposite directions. In the third form, the coils are wound coaxially on the same plane and in opposite directions. In all of these forms, the coils are wound so they will have minimal coupling to the transmitting coil. All of these forms have the disadvantage of being less sensitive to deeply buried targets and having a complicated detection zone when compared to a dipole receive coil.

A new technique is presented for canceling the coupling between the induction coils while maintaining the depth sensitivity and simple detection zone of a dipole coil. Here simple dipole transmit and receive coils are used along with a secondary bucking transformer to cancel the coupling between the coils. A similar use of a bucking transformer was presented for a system operating below 1 kHz in a patent issued in 1972 [5], but the patent does not present a method for compensating for parasitic effects which is crucial at higher frequencies.

## Approach

Figure 1 shows a basic diagram of the system where simple dipole transmit and receive coils are used along with a secondary transformer to cancel the direct coupling between the coils. Here the

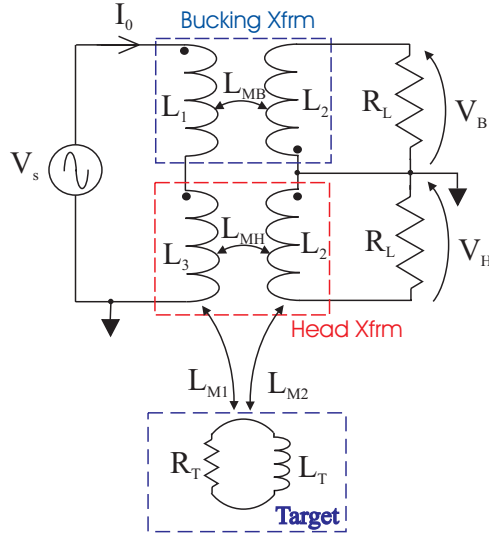


Figure 1. Basic configuration of the technique.

exciting current  $I_o$  passes through the primary coils of both the bucking and head transformers and induces a voltage in the secondary transformers. The voltage induced in the secondary windings of the head transformer depends on its mutual inductance as well as the coupling through the target:

$$V_H = j\omega L_{MH} I_o - \frac{\omega^2 L_{M1} L_{M2}}{R_T + j\omega L_T} I_o.$$

The first term in the equation above is due to the direct coupling between the coils of the head transformer and is generally much larger than the second term which is due to the target. The voltage induced in the secondary windings of the bucking transformer depends only on its mutual inductance:

$$V_B = -j\omega L_{MB} I_o.$$

The response of the target is obtained from the relation

$$R = \frac{V_H + V_B}{V_B} = \frac{j\omega L_{M1} L_{M2}}{L_{MB} (R_T + j\omega L_T)}$$

if we make  $L_{MH}=L_{MB}$ . This is the ideal response (scaled by  $L_{MB}$ ,  $L_{M1}$ , and  $L_{M2}$ ) that we want to obtain with the direct coupling term eliminated. Unfortunately, it is difficult to exactly match the mutual inductances. In figure 3, a method for compensating for the mismatch of the mutual inductances is shown. It is a simple voltage divider that effectively allows us to match the inductances by simply tuning a resistive pot when  $L_{MB} > L_{MH}$ . In addition, the diagram in figure 1 is a good model at low frequencies ( $<1$  kHz), but it omits several important parasitic elements at higher frequencies ( $>1$  kHz).

A diagram with some of the important parasitic elements is presented in figure 2. These parasitic elements significantly reduce the effectiveness of the cancellation obtained above. One method of

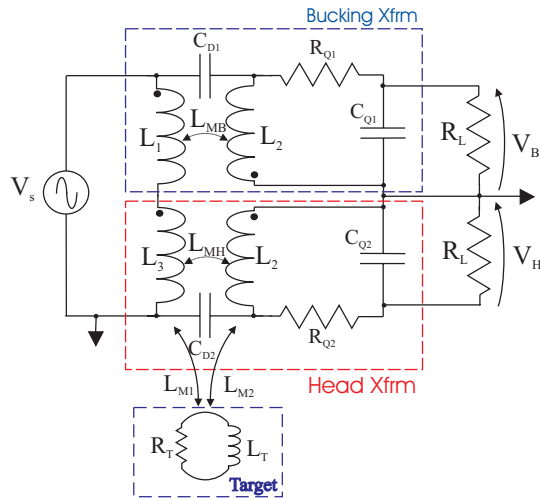


Figure 2. Diagram of EMI sensor with important parasitic elements.

compensation for these parasitics is shown in figure 3.  $R_{Q1}$  and  $R_{Q2}$  are the series resistance of the secondary windings of the transformers, and  $C_{Q1}$  and  $C_{Q2}$  are the inter-winding capacitances of the windings plus the capacitance of the cable connected to the windings. These capacitances and resistances cause a resonance when added to the inductance of the windings.

Since it is impossible to eliminate these capacitances and resistances, the best we can do is to a) make the resulting resonances at frequencies much higher than the operating band of the sensor and b) make the resonant frequency and Q for each of the secondary windings of the transformers as close to each other as possible. For the transformers that we have constructed so far, it has been sufficient to match the Q's of the coils by varying the load impedance imposed on the secondary windings of the transformers, as in figure 3. Here,  $R_{L2}$  is adjusted to match the Q's.

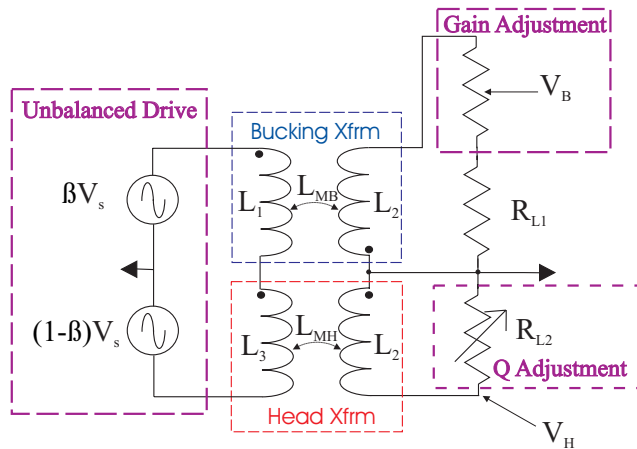


Figure 3. Diagram of EMI sensor with compensating elements.

In figure 2, the capacitances  $C_{D2}$  and  $C_{D2}$ , model the effects of the capacitance between the primary and secondary windings of the transformer. These can be mostly eliminated by proper shielding of the transformers, but they may still be problematic at higher frequencies. In figure 3, an unbalanced drive signal is used to compensate for these capacitances. Two prototypes for the sensor shown in figure 3 were constructed and used to demonstrate these ideas.

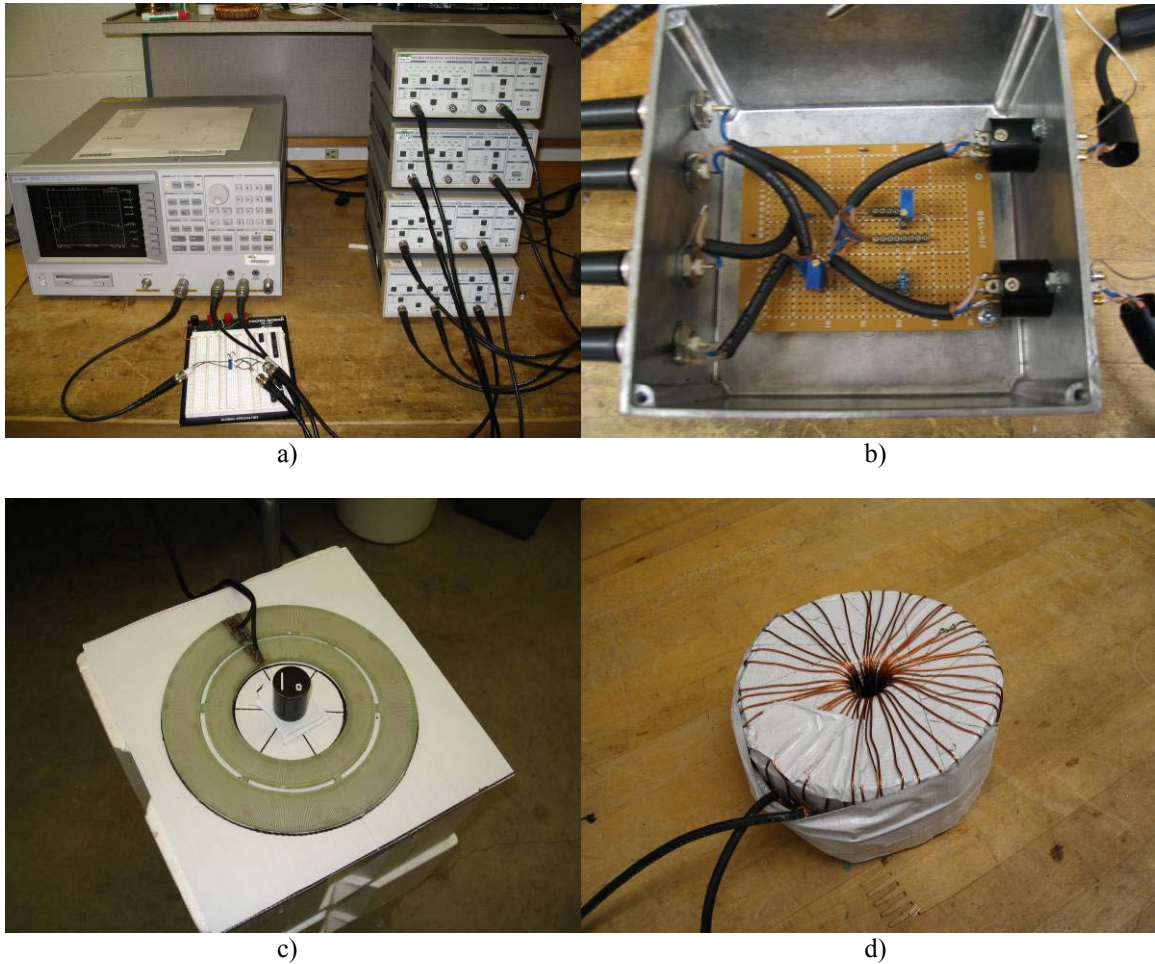


Figure 4. Experimental model to demonstrate the EMI sensor. a) Instrumentation, b) Summing and cancellation network, c) Head transformer, and d) toroidal bucking transformer.

### Experimental Results for Prototype #1

In figure 4, photographs of the components used in prototype #1 are shown. An Agilent model 4395A network analyzer was used to measure the transfer function of the system, and four Stanford Research systems SR560 amplifiers were used in the system. Two SR560s were used as differential preamplifiers to amplify the signals  $V_H$  and  $V_B - V_H$ , and two SR560s were used as power amplifiers for the unbalanced drive signal. These amplifiers were used for the drive as a matter of

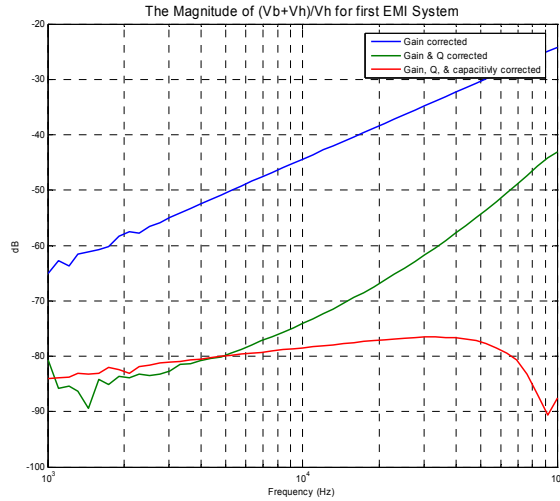


Figure 5. Response of the EMI sensor as a function of frequency.

convenience in that they were readily available, but they can only drive approximately 100mA through the transformers which significantly limits the performance of the system. They will be replaced with stronger amplifiers in the future.

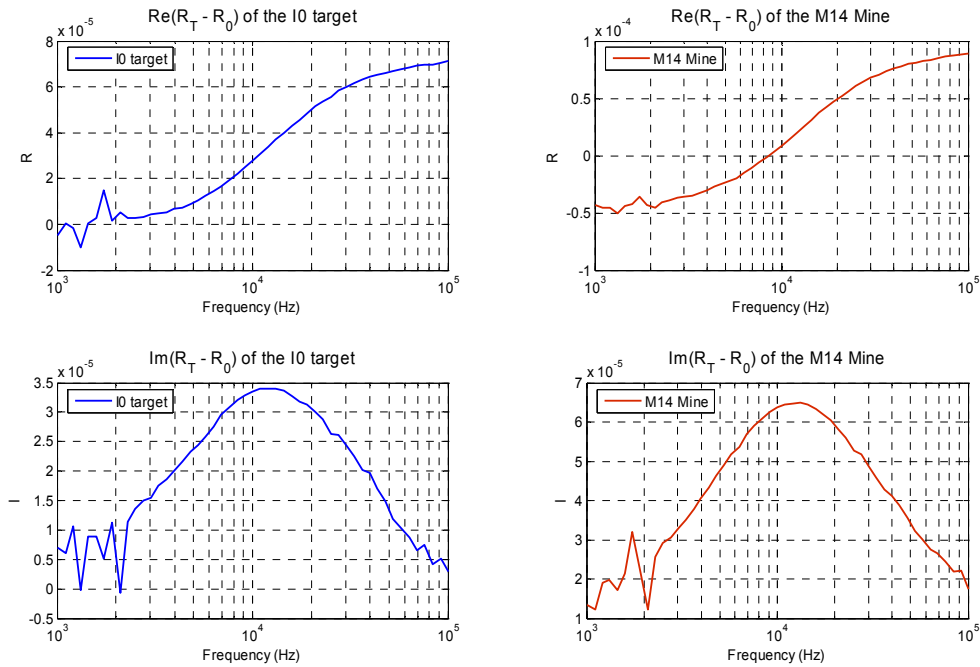


Figure 6. Real and imaginary parts of the response of an I0 target and an M14 landmine as a function of frequency.

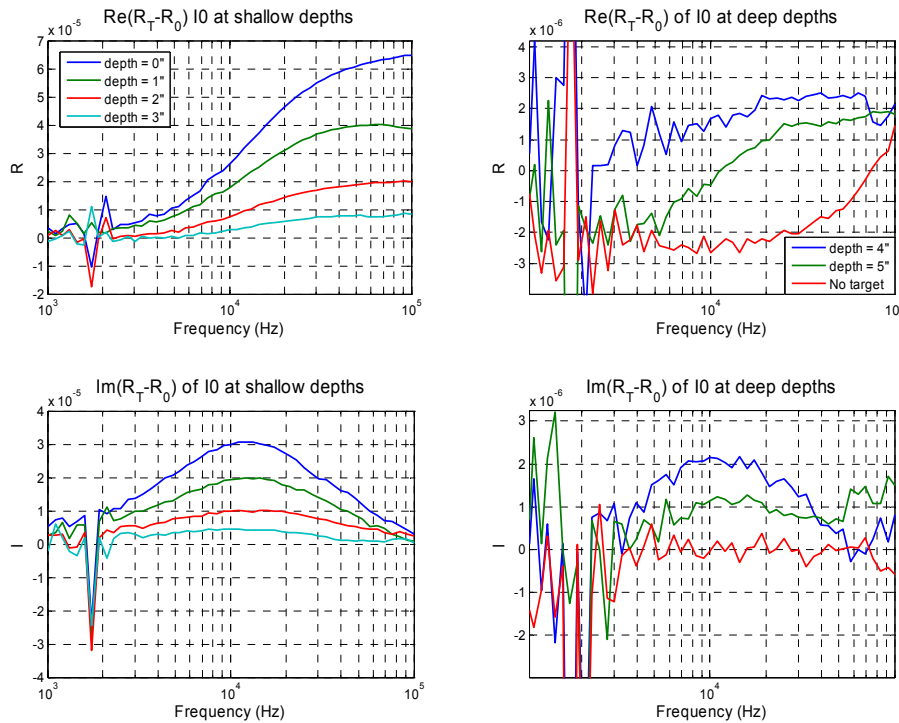


Figure 7. Response of an I0 target as function of frequency at six depths.

The head transformer was made from a FR4 circuit board with 2 oz copper cladding. The primary winding has 20 turns and a radius of 4.75 inches, and the secondary winding has 20 turns and a radius of 3 inch. The traces for the primary winding are 40 mils wide with 10 mil spacing, and the traces for the secondary winding are 20 mils wide with 10 mil spacing. The bucking transformer was made as a toroidal transformer to minimize its sensitivity to metal objects placed in close proximity to it. The toroid has a thickness of 1.78 inches, an inner diameter of 1.75 inches, and an outer diameter of 5.18 inches. The primary winding consists of 118 turns of 18 gauge wire, and the secondary winding consists of 46 turns of 18 gauge wire. The primary and secondary windings are shielded from each other with a metalized Mylar film that is placed between the windings and is grounded. This significantly reduces the capacitance between the primary and secondary windings.

Figure 5 is a graph of the response  $R$  from prototype #1 with no target present as a function of frequency. Ideally the response will be zero with no target present. However, due to the parasitics and imperfect compensation, the response will be non zero. For the top curve, only the gain correction was used which only results in a 25 dB cancellation at 100 kHz. For the middle curve, both gain and Q corrections were used resulting in better cancellation. For the bottom curve, all three corrections were used resulting in more than 75 dB of cancellation for frequencies less than 100 kHz.

Figure 6 shows the real and imaginary parts of the response of the EMI detector for an I0 target and an M14 mine as a function of frequency. To further enhance the cancellation, the response,  $R_o$ , of the sensor with no target present is measured and subtracted from the response,  $R_T$ , with the target present. A single relaxation is seen in these results with the real part of the response of the M14 mine shifted down due to its ferrous content. The noise in the data below 3 kHz is due to power line harmonics. No attempt was made to mitigate the effect of the power line harmonics in this prototype. The effects could be significantly mitigated by using a stronger drive current and choosing the frequencies measures more optimally so that they do not match up with power line harmonics. We believe these results are very good considering the very low drive current:  $I_0 = 75$  mA.

Figure 7 shows the real and imaginary parts of the response of the EMI detector for an I0 target [6] at 6 depths. Also, the response without a target is also shown. These measurements were made with  $I_0 = 75$  mA and a bandwidth of 10 Hz. The response weakens with increasing height above the sand. The effects of the target can be clearly seen at 5 inches with only a 75 mA drive current. The effects of power line harmonics remain clearly evident in the data below 3 kHz.

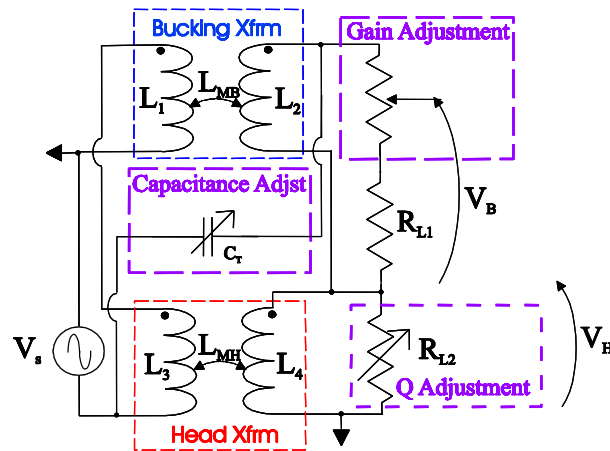


Figure 8. Diagram of EMI sensor with compensating elements for prototype #2.

### Experimental Results for Prototype #2

A second prototype of the sensor was constructed in an attempt to improve its performance. New head and bucking transformers were constructed for this prototype, a different power amplifier is used, and the circuit in figure 3 was simplified to that in figure 8. The new circuit does not need an unbalanced differential power amplifier or differential preamplifiers. A QSC model PLX2402 was used as the power amplifier and is capable of producing 1200W of power with a 2 ohm load. This amplifier is clearly stronger than needed, but it was chosen as a matter of convenience as it was available in our lab and had the appropriate frequency bandwidth. A 2 ohm resistor was placed in series with the primary windings of the transformer to ensure that the impedance of the primary windings was always greater than 2 ohms. Again, the Agilent model 4395A network analyzer was



Figure 9. a) Head transformer and b) toroidal bucking transformer for prototype #2. used to measure the transfer function of the system, and two SR560s were used as preamplifiers to amplify the signals  $V_H$  and  $V_B - V_H$ .

Photographs of the new head and bucking transformers used in prototype #2 are shown in figure 9. The head transformer was made with a form constructed of G10 material. The primary winding has 20 turns and a radius of 5 inches, and the secondary winding has 20 turns and a radius of 4.125 inches. Both windings were made using of 4 parallel strands of 24 AWG wire. The bucking transformer was made as a toroidal transformer to minimize its sensitivity to metal objects placed in close proximity to it. The toroid was made of G10 and has a thickness of 2.25 inches, an inner diameter of 1 inch, and an outer diameter of 5.5 inches. The primary winding consists of 178 turns

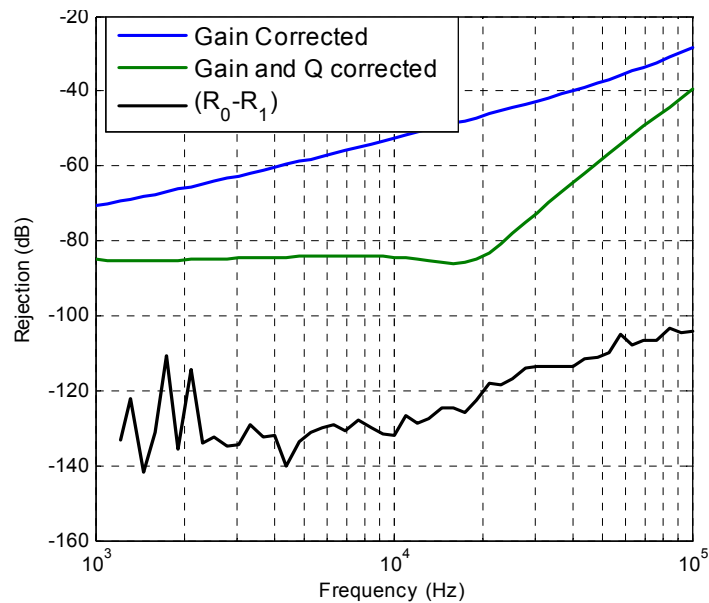


Figure 10. Response of the EMI sensor as a function of frequency.

of 8 parallel strands of 24 AWG wire, and the secondary winding consists of 72 turns of 4 parallel strands of 24 AWG wire. The head transformer is shielded by covering it with a metallized Mylar film. A ring of copper tape is adhered to the Mylar and soldered to the shield of the cables used to drive the head. This significantly reduces the capacitance interactions between the head and the objects to be detected.

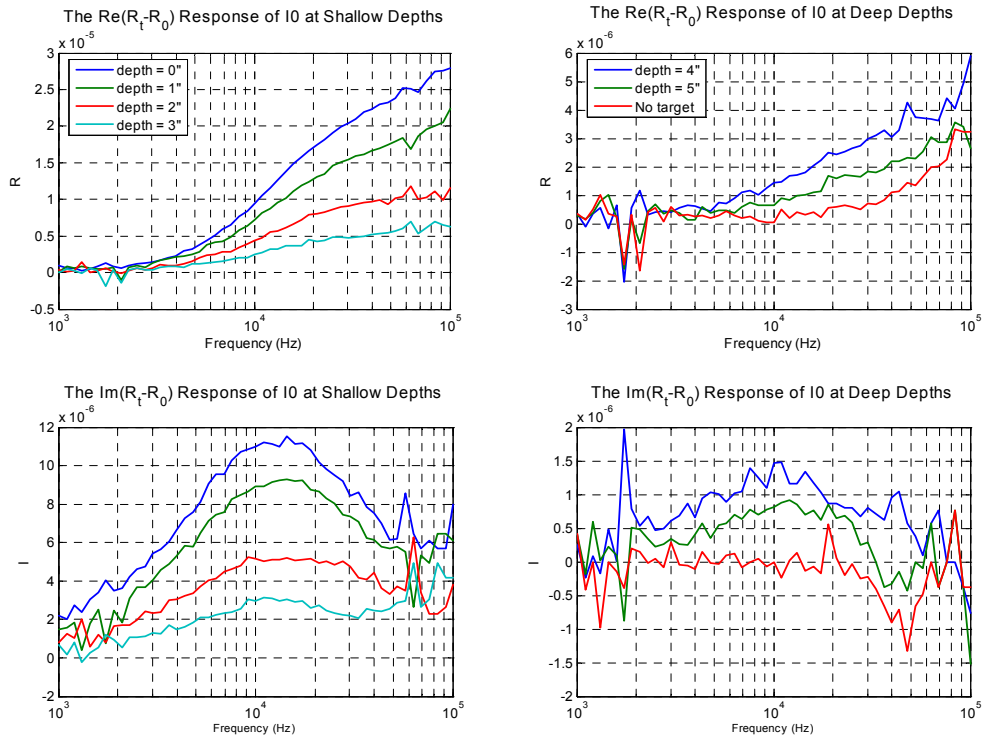


Figure 11. Response of an I0 target as function of frequency at six depths for prototype #2.

Figure 10 is a graph of the response  $R$  from the experimental model with no target present as a function of frequency. Ideally the response will be zero with no target present; however, due to the parasitics and imperfect compensation, the response will be non zero. For the top curve, only the gain correction was used which only results in a 30 dB cancellation at 100 kHz. For the middle curve, both gain and Q correction were used resulting in better cancellation. The capacitive correction proved to be ineffective and unstable and was not used. For the bottom curve, software cancellation is used where the response from one measurement is subtracted from another. With the software correction more than 100 dB of cancellation was obtained for frequencies less than 100 kHz.

Figure 11 shows the real and imaginary parts of the response of the EMI detector for an I0 target at 6 depths. Also, the response without a target is also shown. These responses are seen to be improved over those for prototype #1 at the lower frequencies, and they are degraded at the higher

frequencies. The change in the response is mostly due to the use of a different power amplifier and the resulting change in the drive current.

Figure 12 is a graph of the drive current as a function of frequency. At 1 kHz the current is 0.9A, which is more than ten times greater than that prototype #1, and at 100 kHz the current is 10 mA, which is more than 7 times smaller than that of prototype #1. The variation in current is due to the reactive component of the impedance of the primary winding and the low output impedance of the QSC amplifier. Better matching of the amplifier to the drive coils will result in a good response at all of the frequencies.

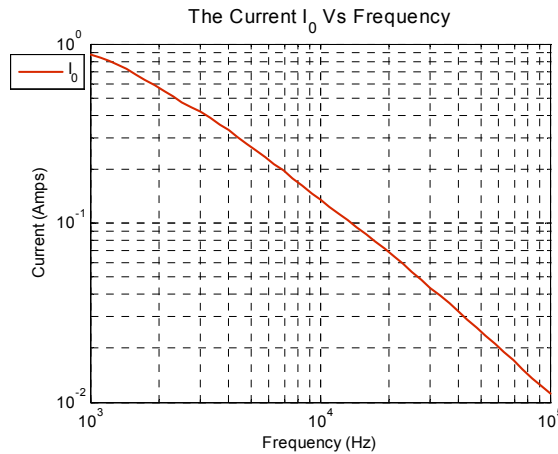


Figure 12. Drive current for prototype #2.

### Sensitivity of Toroidal Transformer to External Metal Objects

A toroidal bucking transformer was chosen because it will mostly contain the magnetic field, resulting in relatively weak fields outside the transformer. The containment of the field will make the transformer relatively insensitive to metal objects outside the transformer. An experiment was performed to verify this. In the experiment, a large piece of metal was placed on the toroidal transformer and the response was measured. The response when the metal is placed on the toroid is compared to that when the metal is placed on the head in figure 13. The response is about 50 dB weaker when the metal is placed near the toroidal transformer than when is near the head transformer..

### Conclusions and Future Work

- A cancellation technique using a bucking transformer and techniques for mitigating some of the parasitic effects were presented. Two prototype models for the system were constructed and used to demonstrate the effectiveness of the cancellation.
- Both systems demonstrated very good sensitivity and response fidelity.

- The bucking transformer was shown to be significantly more insensitive ( $\sim 50$  dB) to external metal objects than the head transformer.
- Tests need to be performed to demonstrate the effectiveness of the capacitive shielding of the head.
- The power amplifier needs to be matched to the system to maximize the performance of the system.
- The network analyzer is not an appropriate tool for making the measurements in a practical system because it is very slow. At these frequencies the signal can be directly digitized and transformed in the frequency domain.
- The measurement frequencies should be chosen to avoid the power line harmonics.
- Field tests need to be performed to demonstrate the performance of this system in the field.

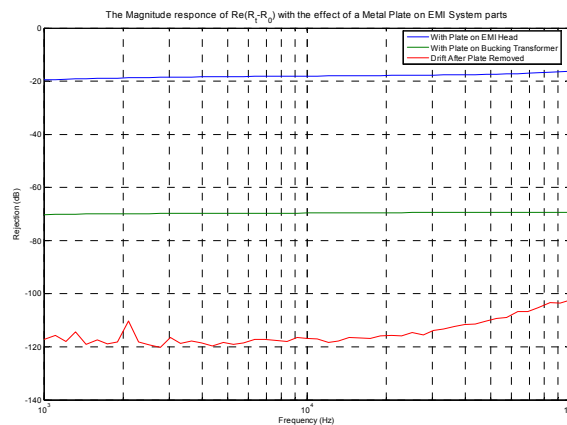


Figure 13. Magnitude of the response of the toroidal bucking transformer and the dipole head transformer to a large metal object..

## References

1. P. Gao, L. Collins, P.M. Garber, N. Geng, and L. Carin, "Classification of Landmine-Like Metal Targets Using Wideband Electromagnetic Induction," *IEEE Transactions on Geoscience and Remote Sensing*, Vol. 38, No. 3, May 2000.
2. L. Collins, P. Gao, and L. Carin, "An Improved Bayesian Decision Theoretic Approach for Land Mine Detection," *IEEE Transactions on Geoscience and Remote Sensing*, Vol. 37, No. 2, March 1999.
3. G. D. Sower and S. P. Cave, "Detection and identification of mines from natural magnetic and electromagnetic resonances," in *Proc. SPIE*, Orlando, FL, 1995.
4. C. E. Baum, "Low Frequency Near-Field Magnetic Scattering from Highly, but Not Perfectly Conducting Bodies," Phillips Laboratory, *Interaction Note* 499, Nov. 1993.

5. G.T. Mallick, Jr. W.J. Carr, Jr., and R.C. Miller, "Multiple Frequency Magnetic Field Technique for Differentiating between Classes of Metal Objects," U.S. Patent 3,686,564, Aug. 22, 1972.
6. L.S. Riggs, L.T. Lowe, J.E. Mooney, T. Barnett, R. Ess, and F. Paca, "Simulants (decoys) for Low-Metallic Content Mines: Theory and Experimental Results," in *Proc. SPIE*, Vol. 3710, Orlando, FL, 1999.

## **Personnel**

Waymond R. Scott, Jr., Professor  
Michael Mulluck, Undergraduate Student

## **Publications**

### **Conference with proceedings**

- Waymond R. Scott, Jr. and Michael Mulluck, "New Cancellation Technique for Electromagnetic Induction Sensors," Proceedings of the SPIE: 2005 Annual International Symposium on Aerospace/Defense Sensing, Simulation, and Controls, Vol. 5794, Orlando, FL, April 2005.
- Waymond R. Scott, Jr. and Michael Mulluck, "New Cancellation Technique for Electromagnetic Induction Sensors," presented at the 8th Annual ARO-JUXOCO Landmine Basic Research Technical Review Meeting, Springfield, VA, Jan. 13, 2005.

## **Report of Inventions**

None